J Biol Phys (2018) 44:1–16
https://doi.org/10.1007/s10867-017-9471-6

ORIGINAL PAPER

Conformations of a charged vesicle interacting with an oppositely charged particle

Hua Duan[1] · Jianfeng Li[1] · Hongdong Zhang[1] · Feng Qiu[1] · Yuliang Yang[1]

Received: 2 August 2016 / Accepted: 12 September 2017 / Published online: 10 October 2017

Abstract Endocytotic and exocytotic processes are usually studied using particle-vesicle systems in theory, but most of them are electroneutral. Nevertheless, charged particle-vesicle systems are much closer to real biological systems. Therefore, wrapping behaviors of a negatively charged vesicle wrapping a positively charged particle are systematically investigated by a series of 2D dynamical simulations in this article. The competition between the elastic bending energy and the electrostatic energy dictates the vesicle configuration and charge distribution. It is found that only for intermediate charge concentrations and small particle sizes a vesicle can completely engulf the particle. When the charge density is high, the interaction between vesicle and particle is unexpectedly weakened by both the hardening effect of the charged membrane and the effective-transportation-frozen effect of the charged components. When the particle is strongly charged, multi-layer folding conformations are observed. These studies may provide important insights into mechanism of endocytotic and exocytotic processes in biological systems.

Keywords Charged vesicle · Nanoparticles · Phase separation

1 Introduction

The plasma membrane separates a cell from its extracellular environment to ensure the stability of the intracellular environment. A major function of the plasma membrane is to control

✉ Jianfeng Li
lijf@fudan.edu.cn

✉ Hongdong Zhang
zhanghd@fudan.edu.cn

[1] The State Key Laboratory of Molecular Engineering of Polymers, Department of Macromolecular Science, Fudan University, Shanghai, 200433, China

the transport of materials into and out of the cell. It is generally called endocytosis and exocytosis, respectively, when large particles enter and exit cells by wrapping. Transport across the plasma membrane has been paid close attention especially in recent decades with the development of particle-based drug delivery system and the investigation of nanotoxicity and viral budding [1–4].

The biological endocytosis progress is very complicated, because there are many influences such as the concentration of the particles, the cell type, the cell environments and the physical-chemical properties of particles. Vesicles possess many similar properties as cells making them ideal model systems [5–13]. It is thus natural for researchers to choose the complex of a vesicle and a particle as a model system to understand the endocytotic and exocytotic processes [14–19]. The membrane-(spherical) nanoparticle model has been studied [16, 20] and it was found that particle wrapping was influenced by both particle-membrane interaction and particle size . In addition to spherical particles, particles with complicated shapes have also been investigated [19, 21–24]. For example, wrapping of ellipsoidal nanoparticles has been found to depend on the aspect ratios of the particles [25, 26]. Even though a lot of works have been devoted to the study of particle-vesicle systems, most of them deal with uncharged particles.

Nevertheless, charged particle-vesicle systems are much closer to real biological systems. Electrostatic interaction between a membrane and a particle has been investigated experimentally [27–30], but the relevant theoretical understandings of this charged system are still far from being complete. Kumar et al. have studied the effect of curvature-induced macroion condensation on the deformation of a charged vesicle [31]. Fošnarič et al. adopted Monte Carlo simulation to study the influence of the charge density of the vesicle on the size of the wrapping region, and they found that the transition from partially wrapped to completely wrapped state is discontinuous [32]. Nevertheless, the influences of particle sizes and charges on the final configuration are still not systematically investigated, mostly because exploring the full phase space of these model parameters is still, somehow, computationally too expensive for full 3D simulations of charged particle-vesicle systems.

In this paper, a charged 2D particle-vesicle system is employed to investigate endocytosis. The influences of particle size, charge density of the vesicle, area fraction of the charges, screening length and mixing free energy are studied using 2D dynamical simulations based on a discrete-variational method proposed by us [33–35]. It should be mentioned that most of the simulations in the current work neglect screening of the Coulomb interaction by counterions. Although catenoids with vanishing bending energy in the neck region cannot form in the 2D case, most of the conclusions in the current study still hold for the 3D case [23, 24, 36, 37]. In addition, the biological structure [38–40] formed by a Schwann cell wrapping over the axon of a neuron can be approximately modeled as the 2D model in this work and it will be shown that this simple model can roughly reproduce the complicated structure of the myelin.

2 Model and simulation

The system is modelled as a negatively charged vesicle interacting with an oppositely charged particle in a 2D plane. In particular, we assume that the charges (naturally, they are carried by the charged amphiphilic molecules) on the vesicle can freely move in the membrane described by a time-dependent Ginzburg Landau (TDGL) equation [33, 41]. In this 2D system, the vesicle shape is represented by $\mathbf{r}(s) = [x(s), y(s)]$ with s parameterizing the vesicle contour. Initially, the 2D vesicle is set to be a circle with radius R_2 and we fix

the perimeter as $2\pi R_2 = 200a$ during deformation, where a is used as unit length in this work. The charged particle is modelled as a full circle with radius R_1.

We assume that the vesicle is composed of two components A and B with the averaged area fractions $\langle\phi_A\rangle$ and $\langle\phi_B\rangle$, respectively. The component B is neutral while the component A is negatively charged with the charge area density ρ_A. The total number of charges on the vesicle is $Q_2 = 2\pi R_2\rho_A\langle\phi_A\rangle$. The particle is positively charged with the charge Q_1, and the charges are assumed to be immobile and uniformly distributed on the particle.

In the initial state, the two components are uniformly distributed on the vesicle. When the positively charged particle is approaching to the vesicle, the vesicle will respond to the particle by adjusting its shape and charge distribution so as to minimize the free energy.

The free energy of this system consists of three parts: the self-energy (excluding the electrostatic interaction) of the vesicle F_1, the electrostatic interaction of charged components of the vesicle F_2 and the electrostatic interaction between the particle and the vesicle F_3. The unit of the energy in 2D system is $e^2/(\epsilon_0 a^2)$ which has been set to 1.0 (e is the elementary charge and ϵ_0 is the vaccum-dielectric constant).

The self-energy (excluding the electrostatic contribution) of vesicle can be expressed as

$$F_1 = \int ds\frac{\kappa}{2}H(s)^2\tau(s) + \int ds\left(-\frac{a_2\phi^2}{2} + \frac{a_4\phi^4}{4} + \frac{b}{2}|\frac{\partial\phi}{\partial s}|^2\right)\tau(s) + \int ds\lambda(s)\tau(s) \quad (1)$$

where the first term accounts for the bending energy where $\tau(s)ds = |d\mathbf{r}(s)/ds|ds$ is the line element [5, 12] and $H(s)$ is the mean curvature of the membrane which is actually just the curvature of the plane curve $\mathbf{r}(s)$. The second term is the Ginzburg-Landau free energy in terms of the order parameter $\phi(s) = \phi_A(s) - \phi_B(s)$, which describes the interaction between components A and B [33, 41]. $\phi_A(s)$ and $\phi_B(s)$ are area fractions of components A and B on the membrane segment s, respectively. In order to focus on the electrostatic interaction, we assume that the mixing free energy is relatively small compared with the electrostatic interaction, so the phenomenological coefficients a_2 is set to 0 and a_4 are set to close to 0 in most of this work. b is set to 1.0 such that A/B interfacial width is of order of a. Note that physically a_4 cannot be set to zero, but we find that a small a_4 would not quantitative change the simulating results so we numerically set this constant to zero in most simulations in this work in order not to introduce too many model parameters. The last term is introduced to impose the local incompressibility on the line element of the 2D vesicle.

Following the Debye-Hückel approximation, the electrostatic interaction of charged components of the 2D vesicle can be written as [42],

$$\begin{aligned} F_2 &= \int_0^{2\pi R_2}\int_0^{2\pi R_2}\int dsds'\frac{\phi_A(s)\phi_A(s')\rho_A^2 e^{-i\mathbf{k}(\mathbf{r}(s)-\mathbf{r}(s'))}}{\mathbf{k}^2+\lambda_D^{-2}}d\mathbf{k}\tau(s)\tau(s') \\ &= \int_0^{2\pi R_2}\int_0^{2\pi R_2} dsds'\phi_A(s)\phi_A(s')\rho_A^2 K_0(|\mathbf{r}(s)-\mathbf{r}(s')|/\lambda_D)\tau(s)\tau(s') \end{aligned} \quad (2)$$

where K_0 is the zero-order modified Bessel function of the second kind. $\lambda_D = \sqrt{(k_B T\epsilon)/(e^2\sum_i Z_i C_i)}$ is the screening length or Debye length of the medium where ϵ is the dielectric constant of the medium and C_i is the concentration of ions with valency Z_i. The dielectric constant is set to $\epsilon = 80\epsilon_0$ in this paper. Note that for the 3D case, $K_0(|\mathbf{r}(s)-\mathbf{r}(s')|/\lambda_D)$ should be replaced by the Yukawa potential $e^{-|\mathbf{r}(s)-\mathbf{r}(s')|/\lambda_D}/|\mathbf{r}(s)-\mathbf{r}(s')|$.

Similarly, the electrostatic interaction between the particle and the vesicle can be expressed as

$$F_3 = \int_0^{2\pi R_2} ds \rho_A \phi_A(s) Q_1 K_0(|\mathbf{r}(s) - \mathbf{r}_p|/\lambda_D)\tau(s) \tag{3}$$

where $\mathbf{r}_p$ is the position vector of the particle center.

The two components are assumed to be mobile and their dynamics can be properly described by the dissipative dynamical equations

$$\frac{\partial \mathbf{r}}{\partial t} = -L_r \frac{\delta F}{\delta \mathbf{r}} \tag{4}$$

and

$$\frac{\partial \phi(s)}{\partial t} = L_\phi \nabla^2 \left[\frac{\delta F}{\delta \phi(s)} \right] \tag{5}$$

where $F = F_1 + F_2 + F_3$ is the total energy of this system. L_r and L_ϕ are two kinetic coefficients [33, 34, 41], which are both set to 1.0 for simplicity. As we mainly focus on the wrapping behavior of this system and the above two equations are employed to obtain the equilibrium state of the system by evolving the equations for a sufficiently long time.

Equations (1-5) can be employed to properly describe the dynamics of the interaction of a 2D charged vesicle and a nanoparticle in a medium with the screening length λ_D. When the screening length λ_D is extremely small, the electrostatic interaction becomes short-ranged and it has been systematically studied previously [32, 33]. When the screening length λ_D is large, the potential function $K_0(r/\lambda_D)$ can be approximated by $\ln(C/r)$ with C some arbitrary constant length and therefore eqs.(2-3) can be reduced to

$$F_2 \approx \int\int ds ds' \ln \left[\frac{R_1}{|\mathbf{r}(s) - \mathbf{r}(s')|} \right] \frac{\rho_A^2 (1 + \phi(s))(1 + \phi(s'))}{4\pi\epsilon(1 + \langle\phi\rangle)^2} \tau(s)\tau(s') \tag{6}$$

and

$$F_3 \approx \int ds \ln \left[\frac{R_1}{|\mathbf{r}(s) - \mathbf{r}_p|} \right] \frac{\rho_A Q_1 (1 + \phi(s))}{2\pi\varepsilon(1 + \langle\phi\rangle)} \tau(s). \tag{7}$$

In order to see the effect of a long-ranged electrostatic interaction, we focus on the case of large screening length in this paper.

In simulations, (4) and (5) are discretized based on a discrete-variational method [33], which has been successfully employed to study both 2D and 3D vesicles [6, 33–35, 43]. The 2D vesicle is numerically represented by 200 discrete points (The corresponding discrete points are numbered in Fig. 1i) and the distance of two neighboring points is constrained to a. Therefore R_2 is about $31.8a$. It should be noticed that, in the following context, the unit charge e has also been rescaled by a, i.e. $\bar{e} = e/a$, and the bending rigidity of vesicle κ is reduced as $\tilde{\kappa}$ ($\tilde{\kappa} = \kappa/k_B T$). The time step Δt is set to 0.01 throughout this work.

3 Results and discussions

3.1 Typical evolution process

We first present typical dynamical evolution pictures of a negatively charged vesicle with total charge $Q_2 = -40.0\bar{e}$ engulfing a positively charged particle with $Q_1 = 30.0\bar{e}$ in Fig. 1.

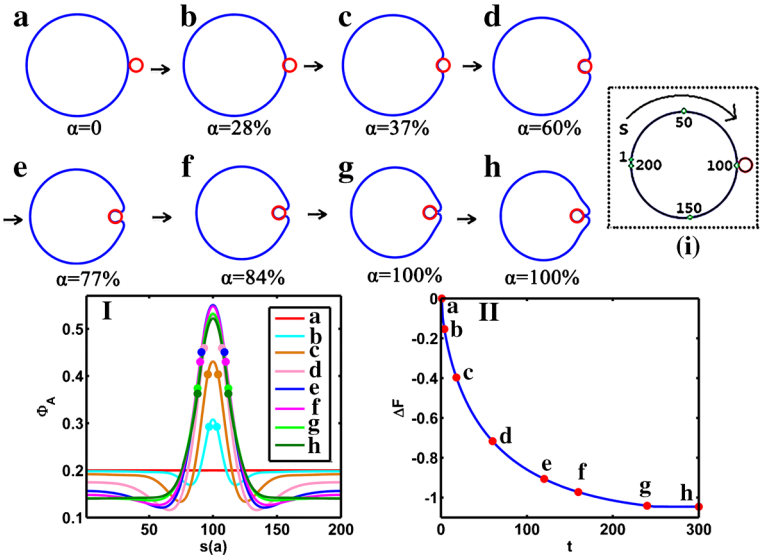

Fig. 1 A typical evolution picture of a charged particle-vesicle system. **a**-**h** Eight snapshots of the particle-vesicle configurations during the evolution where α is the wrapped area fraction of the particle. **i** shows the numbering of discrete points s with $s = 100$ corresponding to the vesicle point closest to the particle in the initial configuration. **I** The corresponding charged component distribution along the contour of the vesicle. **II** Free energy difference curve as a function of the computational time. The unit of the free energy is $e^2/(\epsilon_0 a^2)$. Parameter setting: $\tilde{\kappa} = 0.1$, $\rho_A = -1.0\ e/a^2$, $\langle \phi_A \rangle = 0.2$, $Q_1 = 30.0\ \bar{e}$, $Q_2 = -40.0\ \bar{e}$, $R_1 = 4.0\ a$ and $R_2 = 31.8\ a$. Note that $\tilde{\kappa} \equiv \kappa / k_B T$ is the rescaled bending modulus

It can be seen from Fig. 1a-h that when the particle is placed near the vesicle, the particle will be immediately attracted and easily engulfed by the vesicle due to the electrostatic interaction between these two oppositely charged objects. It is also seen from the free-energy curve (Fig. 1II) that there is no local minimum or meta-stable state during the evolution.

The wrapping process can also be investigated by examing the wrapping area fraction of the particle. Here, the wrapping complex is considered to the complex consisting of the wrapping membrane patch directly contacting the particle and the particle itself. The wrapping area can be read out by measuring the distance between two dots marked on the charge distributions in Fig. 1I. Obviously, the wrapping fraction increases at first (a to g) and then it levels off until a constant value (g-h) has been reached. The shape of the vesicle membrane far away from the wrapping complex is only slightly changed during the evolution indicating that the influence of the particle is quite localized. The membrane patch near the wrapping complex tends to closely contact to the particle surface. Simultaneously, the component A (the negative charge carrier) moves toward to the particle and the vesicle adjusts its shape to further reduce the total free energy. Since the wrapping complex is always positively overcharged (see Fig. 2), the positively overcharged wrapping complex might be able to attract layers to form the folded configuration (see Section 3.3).

Although the charged components will move towards the particle ($s = 100$) because of the electrostatic attractive force between the oppositely charged objects, the concentration of the negatively-charged component A near $s = 100$ will not always increases as the particle approaches. Instead, it decreases a little when $t > 120$ (comparing the curves (f-h) with (e) in Fig. 1I). To quantify this process, we calculate the total charge q of the wrapping complex

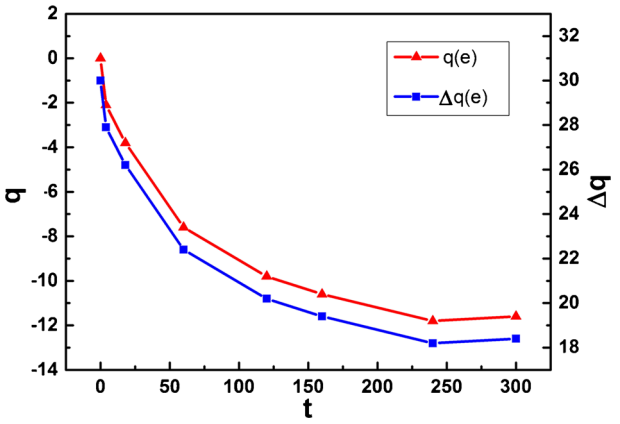

Fig. 2 The total charge q of the wrapping membrane patch directly contacting the particle and the overcharged number Δq of the wrapping complex for the snapshots a-h in Fig. 1. Note $\Delta q = q + Q_1$ with Q_1 the charge of the particle

(q measures the total charge between the two dots marked on the charged distribution line in Fig. 1I) as well as the overcharged number of the wrapping complex Δq ($\Delta q = q + Q_1$ with Q_1 the charge of the particle). When $t = 0$, there is no contact between the membrane and the particle or wrapping complex, so $q = 0$. Then, $|q|$ increases with the increasing wrapping fraction. When the particle is mostly wrapped, $|q|$ reaches its maximum (see Fig. 1g). However, when (g) is evolving to (h), $|q|$ drops a little bit. This abnormal tendency that the peak of the charged concentration decreases at the late stage, is due to the repulsion of gathered negatively charged components A which will slightly push away the negatively charged component on the wrapping membrane patch.

3.2 The equilibrium configurations

By analyzing a series of dynamical simulations in terms of different relative particle sizes R_1/R_2 and charged component fractions $\langle \phi_A \rangle$, a wrapping diagram can be constructed (Fig. 3).

Figure 3 consists of three configurational states: shallow wrapping state (green), deep wrapping state (pink) and complete wrapping state (blue). The corresponding typical complex configurations are also shown in Fig. 3. The shallow wrapping state is defined as a state in which less than 50% of the particle surface is wrapped; the deep wrapping state is defined as the state that more than or equal to 50% of the particle surface but not 100% is enclosed; the complete wrapping state corresponds to the situation where the particle is completely engulfed, including both the asymmetric and the symmetric wrapping states. The symmetric wrapping states have mirror symmetry, and they are wrapped only by one layer of membrane. The asymmetric wrapping states refer to those possessing no mirror symmetry, which are usually encountered if the particle is wrapped by several layers of membranes. We should mention that the wrapping transitions in this diagram are all continuous, which is different from those in 3D case [32].

Note that we have not observed the unwrapped configuration region and the discontinuous transition as observed by Cao et al. [44] and Deserno and Gelbart [16]. The plausible reason is that the vesicle volume is not fixed in this work. For a vesicle with a fixed

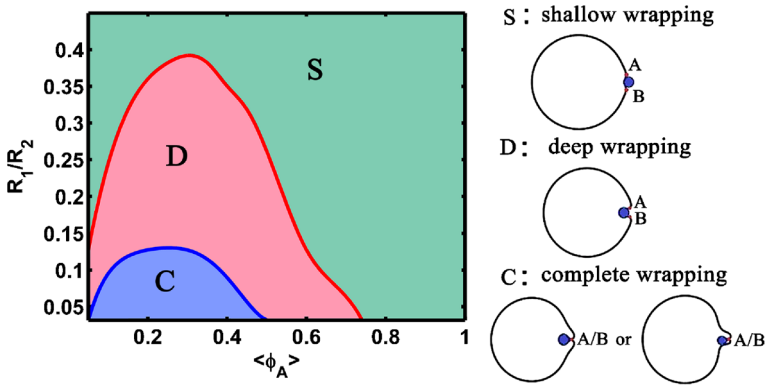

Fig. 3 Possible configurational states of the charged particle-vesicle system with different relative particle sizes R_1/R_2 and different $\langle\phi_A\rangle$. The radius of particle is changed from $1.0a$ to $14.0a$, and $\langle\phi_A\rangle$ is changed from 0.05 to 1.0 with the constant charge density $\rho_A = -1.0e/a^2$. The other parameters of this system are $\tilde{\kappa} = 0.1$, $Q_1 = 30.0\bar{e}$ and $R_2 = 31.8a$

volume, when charged particle is approaching, the vesicle will be reluctant to change its shape to wrap over the particle because it has to change not only the shape of the membrane region near the particle but also the shape of the other membrane patch in order to make the total volume fixed, which will cause a relatively big bending-energy to increase at the beginning of the approaching. The combining effect of this bending-energy increase and the electrostatic energy decrease will result an energy barrier between the transition from the unwrapped to the wrapped states, which will further imply a discontinuous transition between these two states. On the other hand, if the total volume is not fixed, as the charged particle is approaching, the vesicle shape can gradually deform and partly wrap the particle, and the bending energy will not rise too fast, which implies no energy barrier and no discontinuous transition for this case.

The particle size and the charged density are two important factors that determine the final wrapping configurations. Overall, a charged vesicle can completely engulf an oppositely charged particle for an appropriate particle size R_1 and an intermediate electrostatic interaction (see Fig. 3). If the particle is too big then it will be difficult for the vesicle to swallow the particle. When the electrostatic interaction is weak, the attractive interaction is not large enough for the vesicle to wrap over the particle completely. While the electrostatic interaction is too strong, it is also difficult for the vesicle to wrap more particle because of the hardening effect and the effective-transportation-frozen effect of the charged components. So the final equilibrium configuration of the charged vesicle-particle complex is mainly mediated by the competition between the bending energy of the vesicle and the electrostatic energy.

The particle size effect has attracted attention both experimentally and theoretically [20, 21, 45–47]. For example, the particle-(oblate) vesicle system with different volume ratio has been studied by Cao et al. [44]. In the current work, the influence of the particle size is also manifested. As shown in Fig. 3, where R_1/R_2 is between 0.05 and 0.13, the three wrapping states can be observed by tuning $\langle\phi_A\rangle$. The probability of observing complete wrapping states will be smaller for larger particles. When relative particle size R_1/R_2 is bigger than 0.13, only shallow wrapping and deep wrapping states are witnessed and the probability of observing deep wrapping states decreases with increase of R_1. If R_1 is larger than $12.0a$ or $R_1/R_2 > 0.4$, only slightly wrapping states can be observed. The influence of R_1/R_2 is

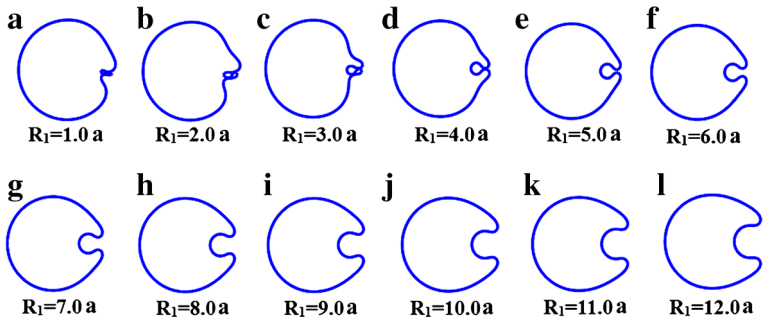

Fig. 4 Equilibrium shapes of the particle-vesicle system with different particle sizes. The particles are not shown in the figure. The relative particle sizes from (**a-l**) are 0.031, 0.063, 0.094, 0.13, 0.16, 0.19, 0.22, 0.25, 0.28, 0.31, 0.35 and 0.38, respectively. The other parameters are $\tilde{\kappa} = 0.1$, $Q_1 = 30.0\bar{e}$, $\rho_A = -1.0e/a^2$, $\langle\phi_A\rangle = 0.2$ and $R_2 = 31.8a$

shown in Fig. 4 for a given $\langle\phi_A\rangle = 0.2$. The wrapped area of particle becomes larger for a bigger R_1/R_2, however, the wrapped fraction of particle will be smaller with increase of R_1/R_2. When the relative particle size is larger, it will cost higher bending energy to wrap the particle completely, and thus the complete wrapping state can hardly form. However, we also have to note that, when the relative particle size is small, the curvature in the wrapping area will be very high and it also costs high bending energy.

Figure 5 also shows the total charge q of the wrapping membrane patch and the overcharged number Δq of the wrapping complex for different particle sizes in Fig. 4. Because the total wrapped area of the particle is increased with the particle size, the total number of charges $|q|$ increases as well. The wrapping complex is positively overcharged for all R_1 and it is heavily extremely overcharged for small particles. Therefore, for small particle it is easier to attract the negatively charged membrane near the wrapping complex to form the asymmetric complicated membrane conformations such as those shown in Fig. 4a-c. Some experimental systems have also reported the influence of particle sizes. For example, Qaddoumi et al. have researched the uptake of PLGA nanoparticles with different sizes (100nm, 800nm and 10μm) in rabbit conjunctival epithelial cell layers, and it is found that

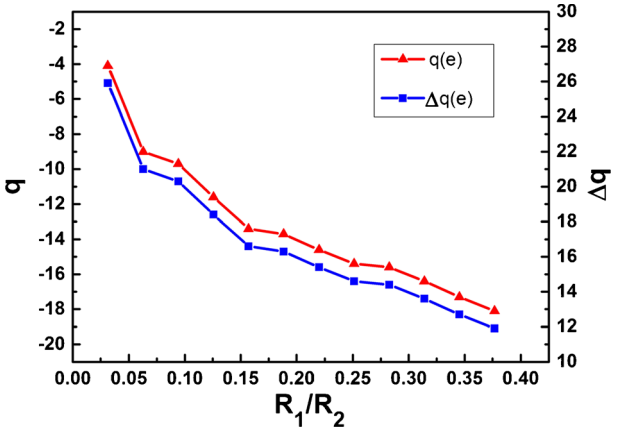

Fig. 5 The total charge q of the wrapping membrane patch directly contacting the particle and the overcharged number Δq of the directly wrapping complex for different relative particle sizes R_1/R_2 in Fig. 4a-l

the nanoparticle with 100nm can be more easily wrapped [48]. This finding qualitatively agrees with our above finding.

The influences of the electrostatic interactions are much more complicated. It is not only because the mechanism is sophisticated but also because there are many ways to affect the overall electrostatic interaction, such as the area fraction of the charged component, the charge density of the charge carrier and the total number of charges on the particle. These factors will contribute to the final intensity of electrostatic interactions. In the following, we try to discuss the subtle differences between these influences. The charged fraction of the vesicle membrane $\langle\phi_A\rangle$ is defined as the averaged area fraction of the charged component A, ρ_A is the charge density of component A which is fixed for the current case, and the total charge number of the vesicle Q_2 is determined by ρ_A and $\langle\phi_A\rangle$, i.e. $Q_2 = 2\pi R_2 \rho_A \langle\phi_A\rangle$.

It is expected that increasing $\langle\phi_A\rangle$ will make the vesicle tend to completely wrap the particle as shown in Fig. 6a-d, since the larger $\langle\phi_A\rangle$ implies stronger attractive interaction between the vesicle and the particle. It is interesting to note that further increasing $\langle\phi_A\rangle$ will enhance the electrostatic repulsion among the negative charge carriers (component A) and result in the hardening of the membrane, and the oppositely charged particle can only be deeply or even shallowly wrapped (Fig. 6e-k). The hardening effect of the membrane can be easily understood in the following way: increasing $\langle\phi_A\rangle$ obviously makes the self-electrostatic repulsive force of the vesicle membrane stronger, and the energy cost for deforming the membrane will be higher. It can be viewed as the increase of membrane rigidity, and this effect has actually been discussed in some other works [49–51]. In addition, the effective-transportation-frozen effect of the near-ceiling area fraction of charged components is also playing a very important role. Because the local concentration of component A cannot exceed 1.0, when $\langle\phi_A\rangle$ is approaching its ceiling value 1.0, the local concentration of A can only vary very little which effectively weakens the apparent transportation of the charged component. When the transporting rate of the charged component is weakened, it is very hard for the vesicle to redistribute the charged component freely to form a complete wrapping state. In the extreme case $\langle\phi_A\rangle = 1.0$ (the curve k on the right part of Fig. 6) the charged component cannot redistribute at all. When $\langle\phi_A\rangle$ is 0.9, the maximum variation of A component near the wrapping complex is only about 0.1.

The charge density ρ_A should be understood as charges carried by a membrane segment with the pure charged component A divided by its length element s, i.e. $\rho_A = dQ/ds$. In the real membrane system, ρ_A measures the ratio of the charge to its cross-section area of a single charged lipid molecule. The total charge Q_2 of the vesicle depends on ρ_A and $\langle\phi_A\rangle$. Although increasing ρ_A and $\langle\phi_A\rangle$ will both increase the total charge of the vesicle,

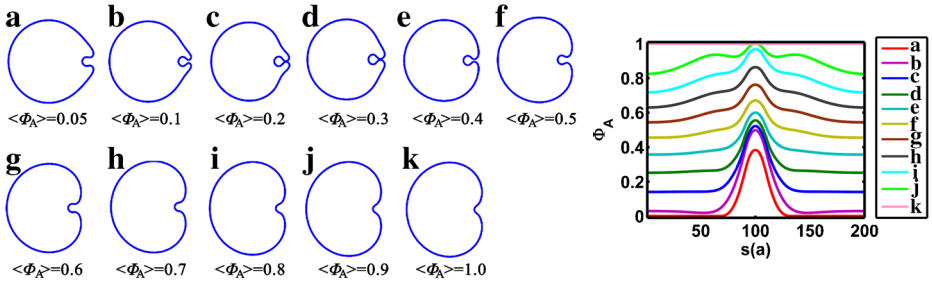

Fig. 6 (Left) Equilibrium shapes of charged vesicles with different $\langle\phi_A\rangle$. (Right) Charged component distribution of the left shapes. From (**a**) to (**k**), the values of $\langle\phi_A\rangle$ are 0.05, 0.1, 0.2, 0.3, 0.4, 0.5, 0.6, 0.7, 0.8, 0.9 and 1.0, respectively. The other parameters are $\tilde{\kappa} = 0.1$, $Q_1 = 30.0\bar{e}$, $\rho_A = -1.0e/a^2$ and $R_1/R_2 = 0.13$

their roles of mediating the final configuration of the complex are slightly different. As discussed above, increasing $\langle\phi_A\rangle$ will first increase the wrapping fraction of the particle but further increasing $\langle\phi_A\rangle$ will decrease the wrapped area of the particle. The influence of ρ_A is more complicated depending on $\langle\phi_A\rangle$. When $\langle\phi_A\rangle$ is small, increasing ρ_A will always make the vesicle wrap more area of particle (Fig. 7A). On the contrary, when $\langle\phi_A\rangle$ is relatively large, increasing ρ_A will make the vesicle reluctant to wrap the particle mainly due to the hardening effect of the charged membrane (Fig. 7B).

3.3 Formation of complicated configurations

The axial symmetry of the vesicle could be broken by the competition between the long-ranged electrostatic interactions and local bending elasticity of the membrane according our previous 3D work [35]. Here, the mirror symmetry of the configuration of the charged vesicle-particle complex can also be broken by increasing Q_1 and the size of vesicle, and some very complicated vesicle configurations can be formed.

Some typical complicated states are shown in Fig. 8. It is seen that, for relatively high Q_1, a normal complete wrapping state (Fig. 8c) will firstly appear. The dynamics will stop at this point if the Coulomb interaction is weak. However, as can be seen from Fig. 8d-l, the vesicle membrane continues to wrap over the particle because of the large attractive interaction. Afterwards, the wrapping part with one double folded layer (Fig. 8f) is gradually formed. Finally, the folded state becomes mirror symmetric again with some parts of the particle surface wrapped by the vesicle membrane twice. The time evolutions of all energetic contributions to the total free energy have also been shown separately in order to present a clear picture about the competition between these different energetic contributions. They are different from previous energy curves that there are two metastable states or local minima during the formation of the folded state. The two metastable states correspond to an ordinarily completely wrapping state (Fig. 8e) and an asymmetric folded state (Fig. 8h), respectively.

When the total particle charge is very high and the vesicle size is large, some very interesting vesicle configurations are observed (Fig. 9). In particular, the configuration of Fig. 9b is at least formally similar to the myelin structure formed by the Schwann cell wrapping over the axon of a neuron. Although, the mechanism of myelination [38–40] is

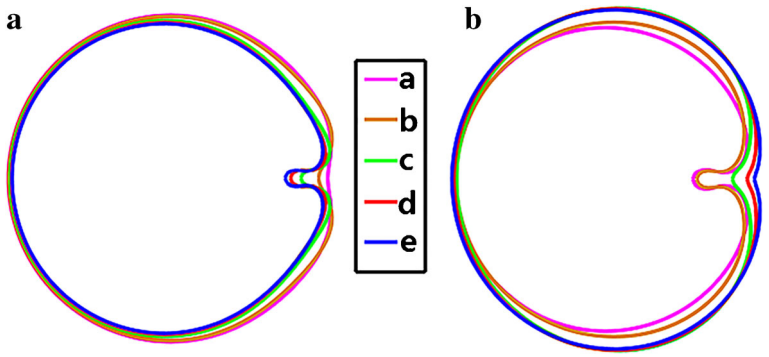

Fig. 7 The equilibrium shapes of the charged vesicle with different ρ_A, and ρ_A from (**a**-**e**) are -0.25, -0.5, -1.0, -1.5 and $-2.0e/a^2$, respectively. **A** $\langle\phi_A\rangle = 0.05$; **B** $\langle\phi_A\rangle = 0.70$. The other parameters: $\tilde{\kappa} = 0.1$, $Q_1 = 20.0e/a$, $R_1/R_2 = 0.063$

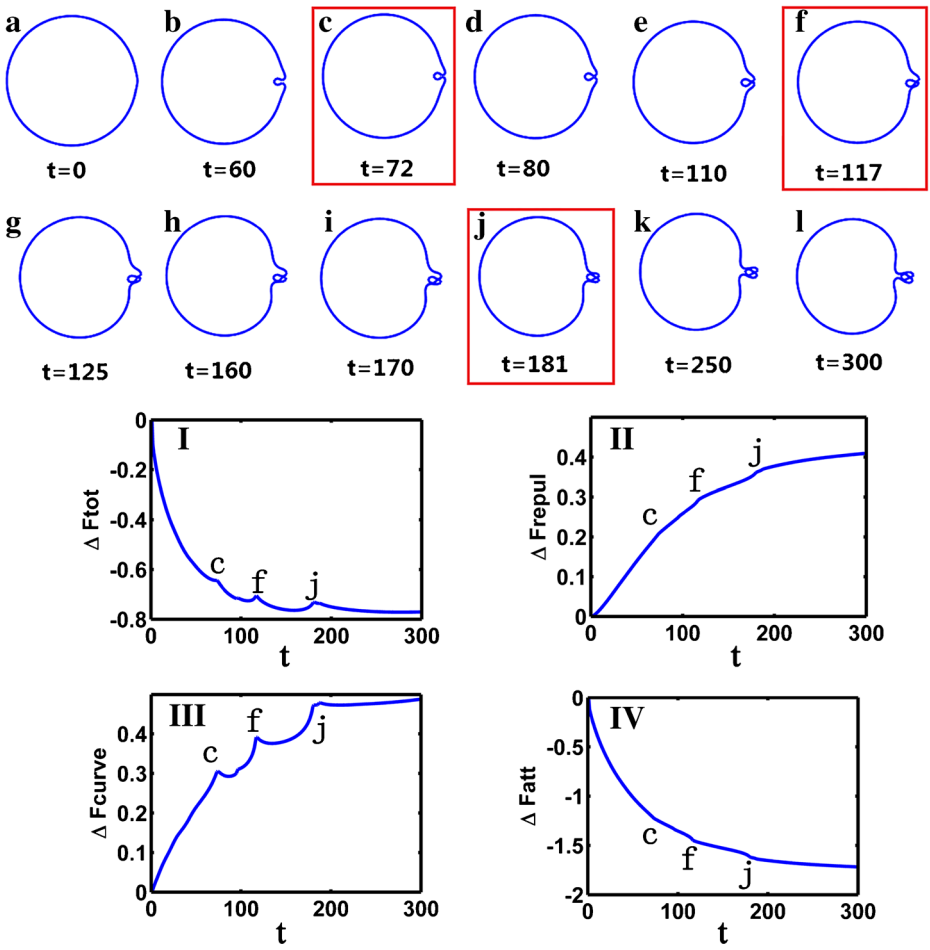

Fig. 8 The formation of the asymmetric wrapping state. **a-l** Twelve snapshots of the vesicle configurations during the evolution. (I) The total energy difference; (II) The repulsive energy difference of the discrete points; (III) The bending energy of the vesicle; (IV) The attractive energy difference between vesicle and particle. The unit of the energy is $e^2/(\epsilon_0 a^2)$. The other parameters are $\tilde{\kappa} = 0.1$, $Q_1 = 35.0\bar{e}$, $\langle\phi_A\rangle = 0.15$, $\rho_A = -1.0e/a^2$, $R_1/R_2 = 0.063$

quite complicated and is not completely understood yet, our result has, at least, provided an alternative point of view about myelination formation.

3.4 Influence of the mixing free energy

The second term in (1) is the Ginzburg-Landau free energy which describes the interaction between components A and B [33, 41]. In order to focus on the electrostatic interaction, the phenomenological coefficients are set to 0 while b is set to 1.0 in the above context, and therefore there is basically no phase separation observed before. Here, we show some preliminary results of non-vanishing a_2 and a_4 in order to demonstrate that the phase separation will greatly complicate the final configurations. Specifically, a_2 and a_4 are both set to 0.2 and b is set to 1.0.

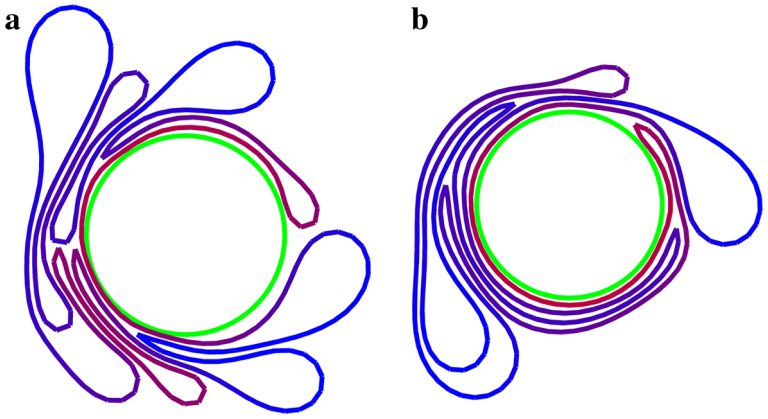

Fig. 9 Two exotic vesicle shapes (meta-stable) are observed when the total particle charge is extraordinarily big ($Q_1 = 400.0\bar{e}$) and the charge density of the lipids is relatively small ($\rho_A = -0.1e/a^2$). Pure blue corresponds to $\phi_A(s) = 0$ on the membrane segment s while pure red $\phi_A(s) = 1.0$ in the figure. The charged particle is denoted by a green circle. The model parameter setting for these two results is the same but with different initial vesicle states: **a**'s initial state is round while **b**'s initial state has been elongated. Parameter setting: $\langle\phi_A\rangle = 0.3$, $\tilde{\kappa} = 0.1$, $2\pi R_2 = 300a$ and $R_1 = 10.0a$

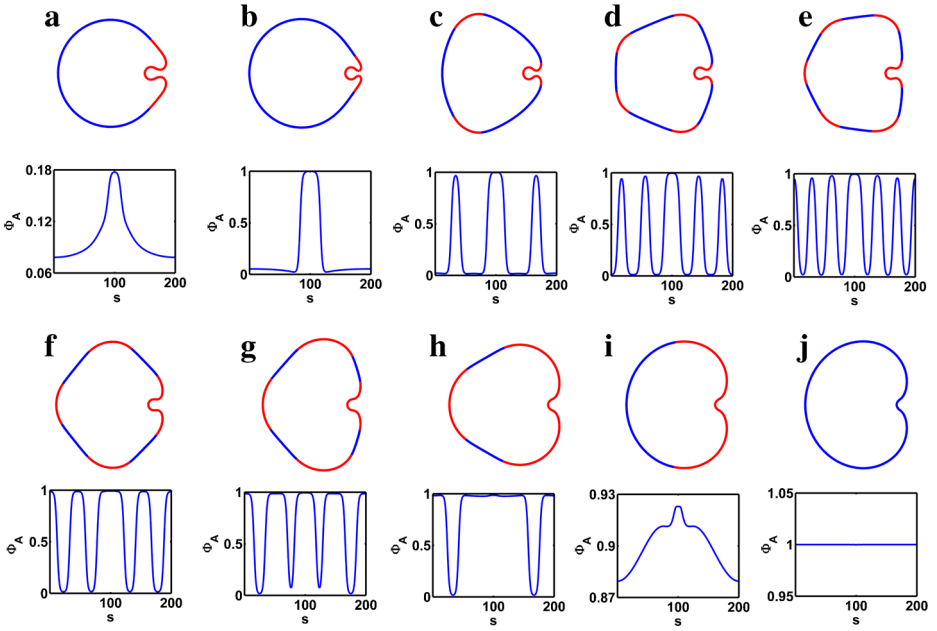

Fig. 10 The equilibrium shapes and their corresponding charged component distributions where the coefficients a_2 and a_4 are set to 0.2. In the equilibrium shapes, the heavily charged membranes are denoted using red curves ($> \langle\phi_A\rangle$) while neutral or slightly charged membranes denoted blue ($< \langle\phi_A\rangle$). $\langle\phi_A\rangle$ from (**a**-**j**) are 0.1, 0.2, 0.3, 0.4, 0.5, 0.6, 0.7, 0.8, 0.9 and 1.0, respectively. The other parameters are $\tilde{\kappa} = 0.1$, $Q_1 = 30.0\bar{e}$, $\rho_A = -1.0e/a^2$, $R_1/R_2 = 0.13$

The equilibrium shapes and their corresponding charged component distributions are shown in Fig. 10 when the mixing free energy is considered. No matter $\langle\phi_A\rangle$ is too big or too small ((a) and (i)), no phase separation can be observed, which is similar to the situation when a_2 is set to 0. When $\langle\phi_A\rangle$ is 0.2, the charged components are mainly gathered around the particle ($s = 100$) and only two phase domains are observed on the vesicle (Fig. 10b). More phase domains show up as $\langle\phi_A\rangle$ increases. For example, when $\langle\phi_A\rangle$ is 0.5 (Fig. 10e, lipids on the vesicle is separated into 12 phase domains. The number of phase domains decreases when further increasing $\langle\phi_A\rangle$ (Fig. 10e-h). Actually, changing a_2 and a_4 will result in more complicated configurations. Here, it is worth mentioning that the phase separated domains might correspond to RAFT formed in the biological cells. However, the systematic investigation of the influence of the mixing free energy is worth conducting and it will be presented in our future work.

3.5 Influence of the screening length

Following the Debye-Hückel approximation [42], the electrostatic interaction can be expressed as (2) and (3). When the screening length λ_D is large enough, (2) and (3) are reduced to (6) and (7) and the above results are obtained in this limit. Figure 11 shows the influence of different screening lengths on the final vesicle configurations. The blue-colored shapes show the equilibrium configurations without screening effects. The red configurations are for the case of $\lambda_D = 100a$ while the green ones for a small screening length $\lambda_D = 5a$.

It is expected that when λ_D is large, the final configurations will be similar to those without screening effect (see blue and red configurations in Fig. 11). It is also expected that when the screening effect is manifested (or λ_D is small), the vesicle will be reluctant to wrap over the particle since the electrostatic interaction between the vesicle and the particle has been weakened by the screening effect. This is the case when $\langle\phi_A\rangle$ is small (see green and blue shapes of (a)-(d) in Fig. 11). Nevertheless, it is a little counterintuitive when $\langle\phi_A\rangle > 0.5$ where the screening effect renders the vesicle more willing to wrap over the particle. This phenomenon can be easily understood by noticing the fact that the screening effect has actually also weakened the hardening effect of the charged membrane, which favors a shallow wrapping state. Overall, counterions not only screen the electrostatic interaction but also 'screen' the other influences such as the influence of the concentration of the charge

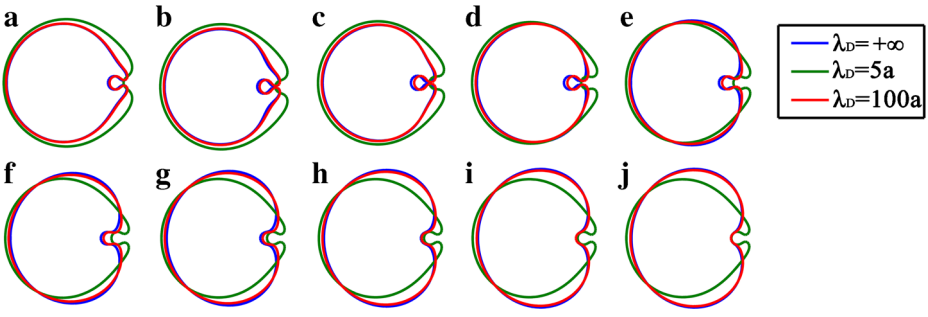

Fig. 11 The equilibrium shapes with different screening lengthes λ_D. $\langle\phi_A\rangle$ from (**a**-**j**) are 0.1, 0.2, 0.3, 0.4, 0.5, 0.6, 0.7, 0.8, 0.9 and 1.0, respectively. The other parameters are $\tilde{\kappa} = 0.1$, $Q_1 = 30.0\bar{e}$, $\rho_A = -1.0e/a^2$, $R_1/R_2 = 0.13$

component, which has effectively enlarged the deep-wrapping window (including complete-wrapping) from $0.05 \leq \langle \phi_A \rangle \leq 0.6$ for $\lambda_D = \infty$ to $0.27 \leq \langle \phi_A \rangle \leq 1$ for $\lambda_D = 5a$.

4 Conclusions

In this paper, the wrapping of a charged particle by a charged vesicle has been systematically studied by a series of 2D simulations. In particular, various influences on this charged vesicle-particle system have been investigated.

The electrostatic interaction between the membrane charged component and the oppositely charged particle would induce the charged components gathering around the particle on the membrane in order to form the wrapping complex, and this will greatly facilitate a complete wrapping state. The complete wrapping state can be observed only when $\langle \phi_A \rangle$ is intermediate and the particle size to vesicle size ratio is small. Higher $\langle \phi_A \rangle$ is not always favorable to achieve complete wrapping due to two effects: (1) the hardening effect of charged membrane; (2) the effective-transportation-frozen effect of charged components. The effective-transportation-frozen effect has been seldom mentioned before. When the particle is heavily charged and relatively small, the oppositely charged vesicle and particle might form a complicated asymmetric state with the particle being wrapped by a few layers of the vesicle membrane. The effect of mixing free energy between the charged and neutral components as well as the screening effect of counterions is also investigated preliminarily.

Although only two-dimension simulations have been investigated in this work, hopefully, this study can still provide a useful hint and meaningful insight into the mechanism of endocytotic and exocytotic processes and some typical structure formation in the biological cells.

Acknowledgments We thank NSFC (Grants No. 21474021, 21534002 and 21574028) for financial support.

Compliance with Ethical Standards

Conflict of interests The authors declare that they have no conflicts of interest.

References

1. Rodriguez, P.L., Harada, T., Christian, D.A., Pantano, D.A., Tsai, R.K., Discher, D.E.: Minimal "self" peptides that inhibit phagocytic clearance and enhance delivery of nanoparticles. Science **339**, 971–975 (2013)
2. Rauch, J., Kolch, W., Laurent, S., Mahmoudi, M.: Big signals from small particles: regulation of cell signaling pathways by nanoparticles. Chem. Rev. **113**, 3391–3406 (2013)
3. Chen, L.K., Bothun, G.D.: Nanoparticles meet cell membranes: probing nonspecific interactions using model membranes. Environ. Sci. Technol. **48**, 873–880 (2014)
4. Mahmoudi, M., Meng, J., Xue, X., Liang, X.J., Rahmand, M., Pfeiffer, C., Hartmann, R., Gil, P.R., Pelaz, B., Parak, W.J., Pino, P.D., Carregal-Romero, S., Kanaras, A.G., Selvan, S.T.: Interaction of stable colloidal nanoparticles with cellular membranes. Biotechnol. Adv. **32**, 679–692 (2014)
5. Ou-Yang, Z.C., Helfrich, W.: Instability and deformation of a spherical vesicle by pressure. Phys. Rev. Lett. **59**, 2489–2488 (1987)
6. Guo, K.K., Li, J.F.: Exploration of the shapes of double-walled vesicles with a confined inner membrane. J. Phys. Condens. Matter. **23**, 285103 (2011)
7. Liu, Y., Chen, Y., Jiang, C., Li, B., Tang, Y., Hu, L., Deng, L.: Depletion effect and biomembrane budding. J. Biol. Phys. **39**, 665–671 (2013)

8. Tu, Z.C.: Challenges in the theoretical investigations of lipid membrane configurations. Chin. Phys. B **22**, 028701 (2013)
9. Li, J.F., Zhang, H.D., Qiu, F., Shi, A.C.: Emergence and stability of intermediate open vesicles in disk-to-vesicle transitions. Phys. Rev. E **88**, 012719 (2013)
10. Lipowsky, R.: Coupling of bending and stretching deformations in vesiclemembranes. Adv. Colloid Interface Sci. **208**, 14–24 (2014)
11. Yin, Y., Lv, C.: Equilibrium theory and geometrical constraint equation for two-component lipid bilayer vesicles. J. Biol. Phys. **34**, 591–610 (2008)
12. Ou-Yang, Z.C., Tu, Z.C.: Overview of the study of complex shapes of fluid membranes, the Helfrich model and new applications. Int. J. Mod. Phys. B **28**, 1330022 (2014)
13. Sreeja, K.K., Ipsen, J.H., Kumar, P.B.S.: Monte Carlo simulations of fluid vesicles. J. Phys. Condens. Matter **27**, 273104 (2015)
14. Koltover, I., Rädler, J.O., Safinya, C.R.: Membrane mediated attraction and ordered aggregation of colloidal particles bound to giant phospholipid vesicles. Phys. Rev. Lett. **82**, 1991–1994 (1999)
15. Noguchi, H., Takasu, M.: Adhesion of nanoparticles to vesicles: a Brownian dynamics simulation. Biophys. J. **83**, 299–308 (2002)
16. Deserno, M., Gelbart, W.M.: Adhesion and wrapping in colloid-vesicle complexes. J. Phys. Chem. B **106**, 5543–5552 (2002)
17. Cao, S.Q., Wei, G.H., Chen, J.Z.Y.: Bending energy of a vesicle to which a small spherical particle adhere: An analytical study. Chin. Phys. B **9**, 098702 (2015)
18. Deserno, M., Bickel, T.: Wrapping of a spherical colloid by a fluid membrane. Europhys. Lett. **62**, 767–773 (2003)
19. Auth, T., Gompper, G.: Budding and vesiculation induced by conical membrane inclusions. Phys. Rev. E **80**, 031901 (2009)
20. Lipowsky, R., Dobereiner, H.-G.: Vesicles in contact with nanoparticles and colloids. Europhys. Lett. **43**, 219–225 (1998)
21. Yang, K., Ma, Y.Q.: Computer simulation of the translocation of nanoparticles with different shapes across a lipid bilayer. Nat. Nanotech. **5**, 579–583 (2010)
22. Dasgupta, S., Auth, T., Gompper, G.: Shape and orientation matter for the cellular uptake of nonspherical particles. Nano Lett. **14**, 687–693 (2014)
23. Mkrtchyan, S., Ing, C., Chen, J.Z.Y.: Adhesion of cylindrical colloids to the surface of a membrane. Phys. Rev. E **81**, 011904 (2010)
24. Chen, J.Z.Y., Mkrtchyan, S.: Adhesion between a rigid cylindrical particle and a soft fluid membrane tube. Phys. Rev. E **81**, 041906 (2010)
25. Dasgupta, S., Auth, T., Gompper, G.: Wrapping of ellipsoidal nano-particles by fluid membranes. Soft Matter **9**, 5473–5482 (2013)
26. Bahrami, A.H., Raatz, M., Agudo-Canalejo, J., Michel, R., Curtis, E.M., Hall, C.K., Gradzielski, M., Lipowsky, R., Weikl, T.R.: Wrapping of nanoparticles by membranes. Adv. Colloid Interface Sci. **208**, 214–224 (2014)
27. Harush-Frenkel, O., Rozentur, E., Benita, S., Altschuler, Y.: Surface charge of nanoparticles determines their endocytic and transcytotic pathway in polarized MDCK cells. Biomacromolecules **9**, 435–443 (2008)
28. Asati, A., Santra, S., Kaittanis, C., Perez, J.M.: Surface-charge-dependent cell localization and cytotoxicity of cerium oxide nanoparticles. ACS Nano **4**, 5321–5331 (2010)
29. Harper, S.L., Carriere, J.L., Miller, J.M., Hutchison, J.E., Maddux, B.L.S., Tanguay, R.L.: Systematic evaluation of nanomaterial toxicity: utility of standardized materials and rapid assays. ACS Nano **5**, 4688–4697 (2011)
30. Ojea-Jiménez, I., García-Fernández, L., Lorenzo, J., Puntes, V.F.: Facile preparation of cationic gold nanoparticle-bioconjugates for cell penetration and nuclear targeting. ACS Nano **6**, 7692–7702 (2012)
31. Sreeja, K.K., Ipsen, J.H., Kumar, P.B.S.: Curvature inducing macroion condensation driven shape changes of fluid vesicles. J. Chem. Phys. **143**, 194902 (2015)
32. Fošnarič, M., Iglič, A., Kroll, D.M., May, S.: Monte carlo simulations of complex formation between a mixed fluid vesicle and a charged colloid. J. Chem. Phys. **131**, 105103 (2009)
33. Li, J.F., Zhang, H.D., Tang, P., Qiu, F., Yang, Y.L.: A discrete, space variation model for studying the kinetics of shape deformation of vesicles coupled with phase separation. Macromol. Theory Simul. **15**, 432–439 (2006)
34. Li, J.F., Zhang, H.D., Qiu, F.: Budding behavior of multi-component vesicles. J. Phys. Chem. B **117**, 843–849 (2013)
35. Li, J.F., Zhang, H.D., Qiu, F., Yang, Y.L., Chen, J.Z.Y.: Conformation of a charged vesicle. Soft Matter **11**, 1788–1793 (2015)

36. Fourcade, B., Miao, L., Rao, M., Mortis, M.: Scaling analysis of narrow necks in curvature models of fluid lipid-bilayer vesicles. Phys. Rev. E **49**, 5276–5286 (1994)
37. Jülicher, F., Lipowsky, R.: Shape transformations of vesicles with intramembrane domains. Phys. Rev. E **53**, 2670–2683 (1996)
38. Salzer, J.L.: Polarized domains review of myelinated axons. Neuron **40**, 297–318 (2003)
39. Sherman, D.L., Krols, M., Wu, L.M.N., Grove, M., Nave, K.-A., Gangloff, Y.-G., Brophy, P.J.: Arrest of myelination and reduced axon growth when schwann cells lack mTOR. J. Neurosci. **32**, 1817–1825 (2012)
40. Monk, K.R., Feltri, M.L., Taveggia, C.: New insights on Schwann cell development. Glia **63**, 1376–1393 (2015)
41. Taniguchi, T.: Shape deformation and phase separation dynamics of two-component vesicles. Phys. Rev. Lett. **76**, 4444–4447 (1996)
42. Sinha, K.P., Thaokar, R.M.: Conformation of charged vesicles: the Debye-Hückel and the low-curvature limit. Eur. Phys. J.E **39**, 73 (2016)
43. Xia, B.K., Li, J.F., Li, W.H., Zhang, H.D., Qiu, F.: A dissipative dynamical method based on discrete variational principle: stationary shapes of threedimensional vesicle. Acta Phys. Sin. **24**, 248701 (2013)
44. Cao, S.Q., Wei, G.H., Chen, J.Z.Y.: Transformation of an oblate-shaped vesicle induced by an adhering spherical particle. Phys. Rev. E **84**, 050901 (2011)
45. Chithrani, B.D., Ghazani, A.A., Chan, W.C.W.: Determining the size and shape dependence of gold nanoparticle uptake into mammalian cells. Nano Lett. **6**, 662–668 (2006)
46. Pan, Y., Neuss, S., Leifert, A., Fischler, M., Wen, F., Simon, U., Schmid, G., Brandau, W., Jahnen-Dechent, W.: Size-dependent cytotoxicity of gold nanoparticles. Small **3**, 1941–1949 (2007)
47. Agudo-Canalejo, J., Lipowsky, R.: Critical particle sizes for the engulfment of nanoparticles by membranes and vesicles with bilayer asymmetry. Soft Matter **9**, 3704–3720 (2015)
48. Qaddoumi, M.G., Ueda, H., Yang, J., Davda, J., Labhasetwar, V., Lee, V.H.L.: The characteristics and mechanisms of uptake of PLGA nanoparticles in rabbit conjunctival epithelial cell layers. Pharm. Res. **21**, 641–647 (2004)
49. Winterhalter, M., Helfrich, W.: Effect of surface charge on the curvature elasticity of membranes. J. Phys. Chem. **92**, 6865–6867 (1988)
50. Lekkerkerker, H.N.W.: Contribution of the electric double layer to the curvature elasticity of charged amphiphilic monolayers. Phys. A **159**, 319–328 (1989)
51. Mitchell, D.J., Ninham, B.W.: Curvature elasticity of charged membranes. Langmuir **5**, 1121–1123 (1989)